

Accuracy of 3D-Printed Models of Aortic Valves – a Comparative Analysis Between Planimetric and Photogrammetric Measurements

Daniel Cernica¹, Diana Opincariu¹, Monica Chițu^{1,2,3}, István Kovács^{1,2,3}, Theodora Benedek^{1,2,3}, Imre Benedek^{1,2,3}

¹ “George Emil Palade” University of Medicine, Pharmacy, Science and Technology, Târgu Mureș, Romania

² 2 Clinic of Cardiology, Emergency Clinical County Hospital, Târgu Mureș, Romania

³ 3 Center of Advanced Research in Multimodal Cardiac Imaging, Cardio Med, Târgu Mureș, Romania

CORRESPONDENCE

Diana Opincariu

Str. Gheorghe Marinescu nr. 50
540139 Târgu Mureș, Romania
Tel: +40 265 215 551
Email: diana.opincariu@yahoo.ro

ARTICLE HISTORY

Received: April 15, 2023
Accepted: May 27, 2023

Daniel Cernica: Str. Gheorghe Marinescu nr. 38,
540139 Târgu Mureș, Romania. Tel: +40 265 215 551,
Email: daniel.cernica@gmail.com

Monica Chițu: Str. Gheorghe Marinescu nr. 50,
540139 Târgu Mureș, Romania. Tel: +40 372 653 100,
Email: iuliacitu@yahoo.com

István Kovács: Str. Gheorghe Marinescu nr. 50,
540139 Târgu Mureș, Romania. Tel: +40 372 653 100,
Email: kov_istvan@yahoo.com

Theodora Benedek: Str. Gheorghe Marinescu nr. 50,
540139 Târgu Mureș, Romania. Tel: +40 372 653 100,
Email: theodora.benedek@gmail.com

Imre Benedek: Str. Gheorghe Marinescu nr. 50,
540139 Târgu Mureș, Romania. Tel: +40 372 653 100,
Email: imrebenedek@yahoo.com

ABSTRACT

Background: 3D printing has changed the paradigm of personalized medicine. Similarly to fingerprints, there are no two identical hearts; consequently, in cardiology, diagnosis and treatment, either medical, interventional or surgical, must be individualized according to the specific problem of a particular patient. The **aim** of this proof-of-concept study was to analyze two measurement methods, the planimetric and the photogrammetric method, in the process of creating a 3D-printed model from cardiac computed tomography angiography images and to evaluate the accuracy of an aortic valve anatomical model. **Material and methods:** Cardiac computed tomography images, obtained from 20 patients with severe aortic stenosis, underwent stereolithographic reconstruction using 3D Slicer to create digital 3D models of the aortic valves. Serial measurements of six key elements of the aortic valvular apparatus were measured on the 3D model and compared to the measurements taken on the 2D computed tomography images. **Results:** The differences between the two measurement methods were sub-millimetric in case of the left ventricular outflow tract and the sinotubular junction, and 1.386 mm for the left sinus of Valsalva ($p = 0.0412$), 0.3476 mm for the right sinus of Valsalva ($p = 0.1874$), and 0.6905 mm for the non-coronary Valsalva sinuses ($p = 0.1353$). Sinus heights were also similar, with a difference of 0.0119 mm ($p = 0.6521$). **Conclusion:** In this study, the results of digital photogrammetry were superimposable to those of computed tomography scan measurements. The accuracy of each 3D-printed model depends on geometric complexity, the level of training of the personnel, and on the resources of each 3D printing laboratory.

Keywords: validation, 3D printing, aortic valve, additive manufacturing, anatomical models

INTRODUCTION

Similarly to fingerprints, there are no two identical hearts. Consequently, diagnosis and treatment — either medical, interventional, or surgical — should be individualized according to the specific problem of a particular patient. Cardiovascular imaging has gone through an impressive technological progress in recent years, 3D-printed cardiac imaging currently being the cornerstone of the modern management of patients with complex cardiovascular pathology. 3D printing has opened up new perspectives and opportunities in interventional and surgical fields.¹ The applicability of 3D printing is extensive and includes congenital heart disease, mitral and aortic valvulopathies (e.g., transcatheter aortic valve implantation, TAVI), valvular prosthetics (closure of paraprosthetic leaks), and structural heart disease (closure devices for ventricular defects or closure of the left atrial appendage).² The preprocedural work-up could benefit substantially from 3D printing, especially by simulating the implantation of devices of different sizes. The ongoing French observational register FFPP-Print has highlighted its benefits by demonstrating shorter operating times, a significant reduction in the number of prostheses used for each patient, and the ability to assess the risk of complications. Apart from complex procedures, 3D printing can find its utility in anticipating rare but serious complications that can occur during transcatheter interventions such as TAVI. Studies clearly show that morbidity and mortality rates are lower than with conventional surgery for high- or intermediate-risk patients, but this risk should be analyzed individually for each patient.³

In this proof-of-concept study, we aimed to investigate whether 3D models created from cardiac computed tomography (CT) images could have comparable dimensions to the native valve apparatus and to study the feasibility of using 3D-printed aortic valves in simulations of transcatheter implantation.

MATERIAL AND METHODS

Study participants

This was a cross-sectional observational study that included 20 patients with severe aortic stenosis who underwent preprocedural planning for TAVI. The study was conducted from January 2020 to December 2021. Exclusion criteria included the presence of a high degree of aortic valve calcifications, irregular heart rate or inability to achieve a heart rate < 65 bpm, or any other conditions that may have interfered with image acquisition. Clinical, echocardiographic,

and laboratory examinations, as well as contrast-enhanced cardiac CT and computed angio-tomography of the lower limbs were performed for all patients. For cardiac CT image acquisition, a retrospective ECG-gated scanning protocol was used, with intravenous high-concentration iodine contrast agent, at a heart rate of <65 bpm. Patients with increased heart rate were administered beta blockers or ivabradine before scanning. All CT scans were performed using SOMATOM Definition 128-slice CT equipment (Siemens Healthcare, Germany). Patients with inadequate valvular and vascular anatomy for TAVI, as well as sub-optimal quality of CT images were excluded. All study procedures were performed according to good clinical practice (GCP) guidelines and the Declaration of Helsinki, and were approved by the ethics committee of the institution where the study was conducted. All study participants signed an informed consent prior to enrollment.

Stereolithographic model generation—from CT scan to digital model

As part of an ongoing research project at the “George Emil Palade” University of Medicine, Pharmacy, Science and Technology of Târgu Mureș, patient-specific digital models were generated to determine the feasibility of 3D-printed aortic valve models for preprocedural planning.

Image post-processing was performed for all individual CT images to obtain the stereolithographic reconstruction of the models used for 3D printing. The Digital Imaging and Communications in Medicine (DICOM) datasets that were analyzed had a slice thickness of 0.60 mm using a medium smooth kernel. All image reconstructions were performed by a single analyst using 3D Slicer, an open-source offline image computing platform for image analysis and scientific visualization.

The first step in the stereolithographic processing of 3D models consisted in integrating the imaging data into 3D Slicer and delineating the regions of interest (ROIs) on anatomical structures (Figure 1). The second step consisted in the so-called ‘segmentation’, based on the intensity of the studied structures, measured in Hounsfield units (HU). For example, for cardiac structures, a range of 230 HU to 15 HU was used. The third step consisted in rapid prototyping, achieved by placing spatial markers at the level of fluid structures called ‘blood pool’, which enabled us to differentiate the contrast agent from muscle or fibrous structures by subtraction based on Boolean algorithms (Figure 2). Segmentation time was approximately 60–80 min per model, as described previously.⁴ The fourth step consisted in transforming DICOM files into .STL (Standard Tessell-

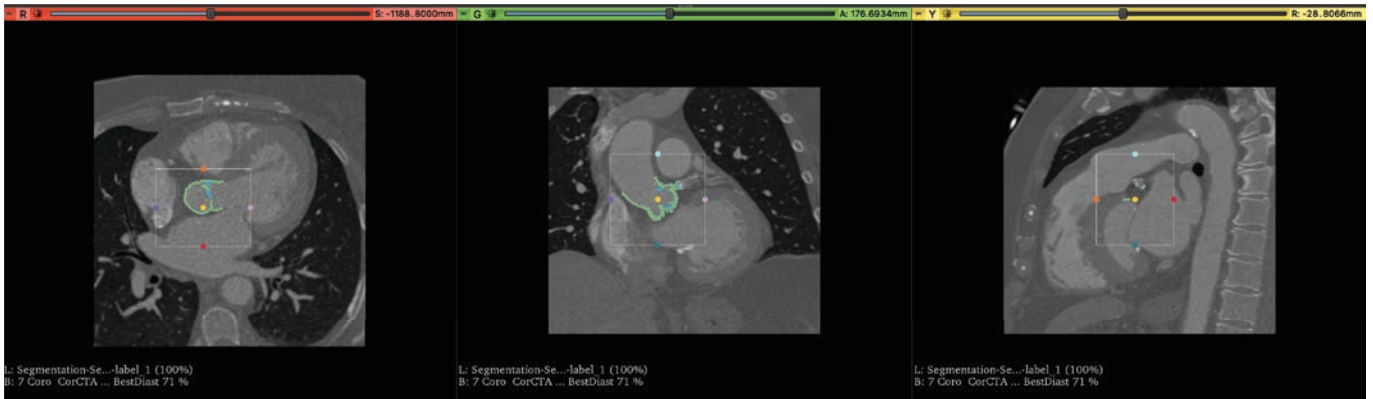


FIGURE 1. Segmentation of ROIs at the level of the aortic valve (green)

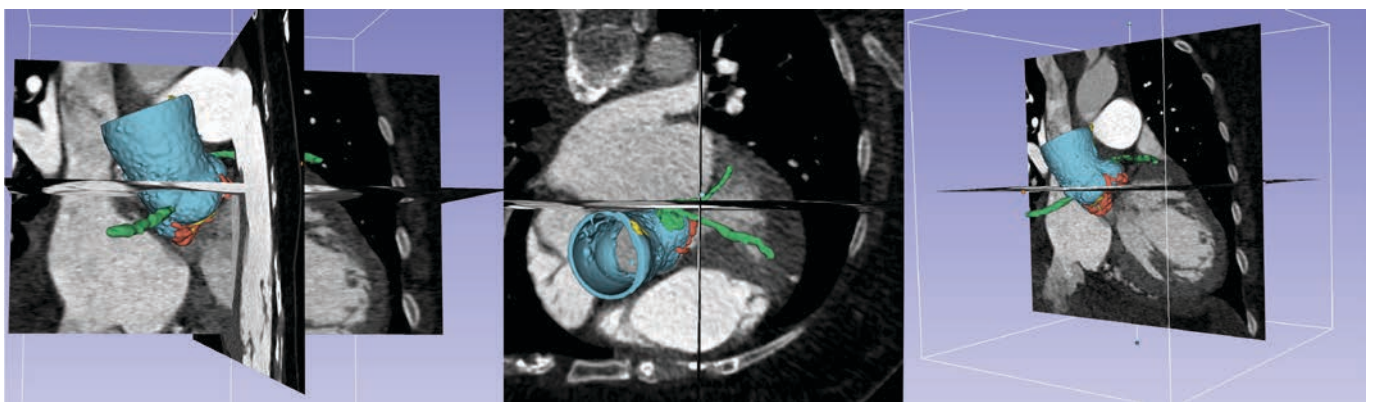


FIGURE 2. Segmentation – selection of “blood pool” at the level of the aortic valve (green)

lization Language) files used in 3D printing. The 3D digital dataset was converted into a virtual 3D model (Figure 3), and automatic or manual cropping functions (“crop mask”) were applied. The 3D model obtained after the segmentation process consisted of a structure of triangular facets with semi-finished surface.

Although the model processed in STL format could have been printed at this stage, anatomical models generally require an additional stage. Optimization of the model can be achieved using computer-aided design (CAD) in

programs such as Autodesk Meshmixer (Autodesk Inc., San Rafael, CA, USA). This step involved remeshing, a process that optimizes the model’s geometry and density, and tessellation, a process that optimizes the triangular facets of the mosaic that make up the digital 3D model (Figure 4). Post-processing time using CAD software was approximately 60 min per model.

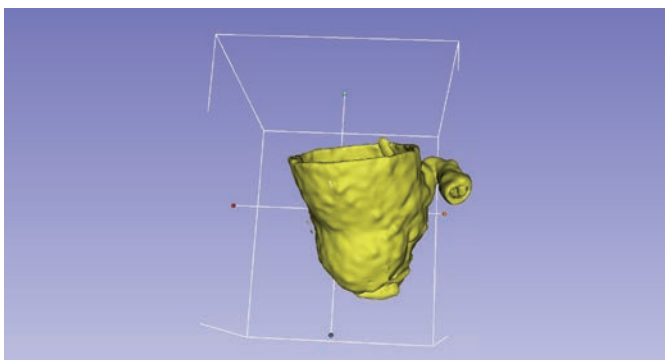


FIGURE 3. Digital 3D model of the aortic valve, ascending aorta and coronary arteries, lateral view

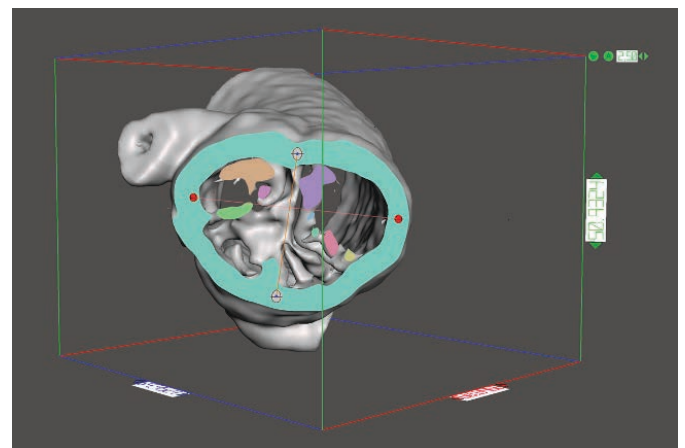


FIGURE 3. Digital 3D model of the aortic valve, ascending aorta and coronary arteries, lateral view

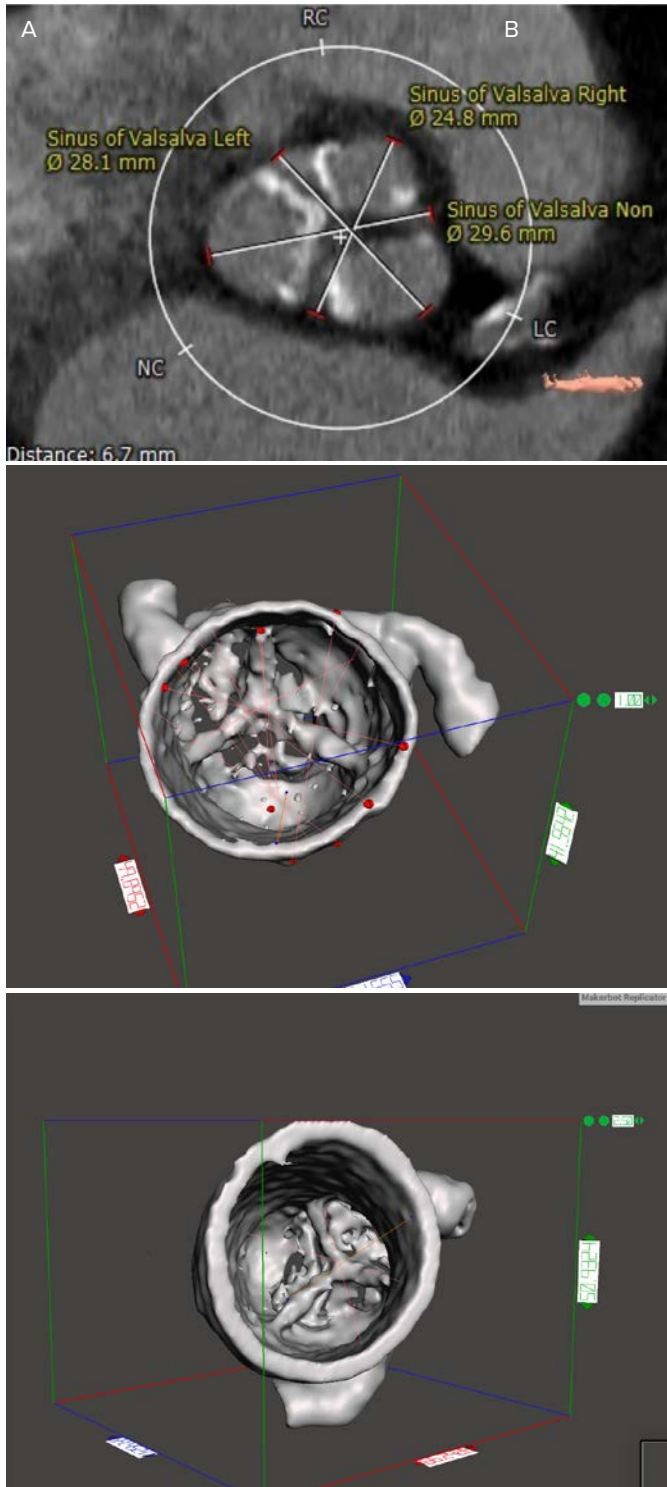


FIGURE 5. Measurement methods: planimetric (A) and photogrammetric (B, C)

In the final step, a digital snapshot of the CT scans, along with an embedded report of the measurements, was exported to Autodesk Meshmixer and overlaid on the STL file for reference to ensure that the STL file features were measured at the same location as the digital mea-

surements. We identified six elements of the aortic valvular apparatus that were accessible to be measured and obtained a total of 13 linear measurements. The following parameters were measured on both the multiplanar dataset CT model and the STL digital model of the aortic valve complex:

- the origin of the left coronary artery (LCA) and the right coronary artery (RCA);
- right, left and noncoronary sinuses of Valsalva;
- the diameter of the aortic annulus;
- the left ventricle outflow tract (LVOT);
- the ascending aorta;

Landmark measurements on digital models

After finalizing image post-processing and the 3D-printed models, we conducted serial measurements of several parameters used for TAVI preprocedural planning. As an initial step, we performed one set of measurements on the 2D cardiac CT dataset using direct planimetry and multiplanar reconstruction in Syngo.via software (Siemens Healthcare, Germany), during mid-systole, at approximately 240–330 ms (Figure 5).

To ensure accuracy, all anatomic analyses were performed using the center line of the lumen as reference. Then, the effective measurement was calculated as the arithmetic mean of minimum and maximum values.

We measured key elements in the STL file in a 3D AutoCAD program and used vertex-to-vertex analysis to compare them to digital measurements of 3D aortic valve models (photogrammetric method).

Statistical analysis

Statistical analysis of the recorded data was performed using GraphPad Prism version 8.4.3 (GraphPad Software, San Diego, CA, USA).

After testing for normality using the D’Agostino–Pearson algorithm, quantitative data were expressed as mean \pm standard deviation. Paired data were compared using Student’s t test or the Wilcoxon matched-pairs signed rank test, and differences between means were calculated using the Bland–Altman method, with 95% confidence intervals.

Intra-class correlation was analyzed by calculating the Pearson correlation coefficient for normally distributed data and the Spearman coefficient for non-normal distribution. A p value of <0.05 was considered statistically significant.

TABLE 1. General clinical characteristics of the study population

Parameter	Value
Age, years	72.43 ± 4.96
Males, n (%)	10 (52%)
Smoking, n (%)	8 (40%)
Arterial hypertension, n (%)	15 (75%)
Obesity, n (%)	11 (55 %)
Dislipidemia, n (%)	5 (25%)
Diabetes mellitus, n (%)	6 (30 %)
Chronic kidney disease, n (%)	9 (45 %)
Coronary artery disease, n (%)	17 (85%)
Left ventricular systolic dysfunction, n (%)	5 (25%)
Bicuspid valve stenosis, n (%)	2 (10 %)
Degenerative aortic stenosis, n (%)	18 (90 %)
Aortic regurgitation, n (%)	15 (75 %)

RESULTS

The general characteristics of the study population are listed in Table 1. Mean age was 72.43 ± 4.96 years, the majority of the patients were men, and the most frequent cause of aortic stenosis was degenerative aortic stenosis, followed by congenital bicuspid valve with degenerative features.

The measurement of digital and 3D-printed models

For the evaluation of the valvular and perivalvular apparatus, anatomical structures were analyzed separately. The comparative analysis of planimetric and photogrammetry measurements, as well as the differences between mea-

surement values provided by the two methods are listed in Table 2. The difference regarding the height of the coronary ostium was 0.0238 mm for the LCA ($p = 0.9022$) and 0.2095 mm for the RCA ($p = 0.4349$). The measurements of the aortic annulus showed a difference between minimum values of 1.0000 mm ($p = 0.1033$) and between maximum values of 0.5700 mm ($p = 0.3315$). Although the differences between planimetric vs. photogrammetric diameters of the sinuses of Valsalva were larger for the left sinus of Valsalva (1.386 mm, $p = 0.0412$), they were not significant for the right sinus of Valsalva (0.3476 mm, $p = 0.1874$) and the noncoronary sinus of Valsalva (0.6905 mm, $p = 0.1353$). Sinus heights were similar with the two methods, with a difference of 0.0119 mm ($p = 0.6521$). Ascending aorta measurements were also similar, with a difference between minimum values of -0.0523 mm ($p = 0.7854$) and between maximum values of 0.2571 mm ($p = 0.3373$). Measurements of the sinotubular junction were comparable, with a difference between minimum values of 0.0285 mm ($p = 0.9564$) and between maximum values of 0.3714 mm ($p = 0.3273$). LVOT assessment showed no differences between the two methods, with a difference between minimum values of 0.7238 mm ($p = 0.1381$) and between maximum values of 0.3714 mm ($p = 0.3315$).

The reliability of 3D models – intraclass correlation coefficients

The intraclass correlation coefficients were statistically significant for all measurements, indicating good reliability of 3D CT measurements (Table 3). The highest correlation

TABLE 2. Comparison of planimetric and photogrammetric measurements

Landmark	Planimetric (mean ± SD)	Photogrammetric (mean ± SD)	Difference between means	p value
LCA height, mm	14.71 ± 3.543	14.69 ± 3.676	0.0238	0.9022
RCA height, mm	17.50 ± 3.665	17.29 ± 3.694	0.2095	0.4349
Left sinus of Valsalva diameter, mm	32.93 ± 4.289	31.55 ± 4.822	1.3860	0.0412
Right sinus of Valsalva diameter, mm	30.11 ± 4.320	29.76 ± 4.266	0.3476	0.1874
Noncoronary sinus of Valsalva diameter, mm	32.77 ± 3.827	32.08 ± 3.231	0.6905	0.1353
Ascending aorta min diameter, mm	34.02 ± 3.414	33.97 ± 3.532	0.0524	0.7854
Ascending aorta max diameter, mm	35.52 ± 3.301	35.26 ± 3.663	0.2571	0.3373
Sinotubular junction min diameter, mm	29.24 ± 4.792	29.21 ± 5.251	0.0286	0.9564
Sinotubular junction max diameter, mm	30.21 ± 4.170	29.84 ± 4.096	0.3714	0.3273
Aortic annulus min diameter, mm	21.38 ± 3.329	22.38 ± 4.577	1.0000	0.1033
Aortic annulus max diameter, mm	27.49 ± 3.450	28.07 ± 3.984	0.5762	0.3315
LVOT min diameter, mm	21.32 ± 4.962	22.04 ± 5.516	0.7238	0.1381
LVOT max diameter, mm	28.83 ± 3.647	29.20 ± 4.232	0.3714	0.4093
Sinus of Valsalva height, mm	24.55 ± 4.979	24.43 ± 4.519	0.1190	0.6521

TABLE 3. The intraclass correlation between measurements obtained from the two methods

Landmark	Correlation coefficient (r)	95% confidence interval	p value
LCA height, mm	0.9712	-0.4230 to 0.3753	0.9022
RCA height, mm	0.9464	-0.7580 to 0.3390	0.4349
Left sinus of Valsalva diameter, mm	0.8022	-2.710 to -0.06124	0.0412
Right sinus of Valsalva diameter, mm	0.9631	-0.8788 to 0.1835	0.1874
Noncoronary sinus of Valsalva diameter, mm	0.8472	-1.616 to 0.2350	0.1353
Ascending aorta min diameter, mm	0.9692	-0.4483 to 0.3436	0.7854
Ascending aorta max diameter, mm	0.9460	-0.8027 to 0.2884	0.3373
Sinotubular junction min diameter, mm	0.8932	-1.105 to 1.047	0.9564
Sinotubular junction max diameter, mm	0.9161	-1.143 to 0.4001	0.3273
Aortic annulus min diameter, mm	0.8146	-0.2222 to 2.222	0.1033
Aortic annulus max diameter, mm	0.7544	-0.6314 to 1.784	0.3315
LVOT min diameter, mm	0.9214	-0.2535 to 1.701	0.1381
LVOT max diameter, mm	0.8789	-0.5479 to 1.291	0.4093
Sinus of Valsalva height, mm	0.9731	-0.6616 to 0.4235	0.6521

min, minimum; max, maximum

coefficient was obtained for the height of the sinus of Valsalva (Figure 6).

DISCUSSION

This study was a proof of concept that aimed to compare the planimetric and the photogrammetric measurement method in the process of creating a 3D-printed model from cardiac CT angiography images. Another aim of the study was to verify the accuracy of each step of this process as part of quality assurance and to discuss the challenges encountered with each method. The main findings of the study are that 3D-printed models provide a feasible, non-invasive method to assist the 3D visualization of patient-specific aortic root anatomy, and that 3D modeling represents a new opportunity to plan in situ device placement during transcatheter aortic valve replacement. Furthermore, 3D modeling may complement traditional methods

used to predict and potentially avoid complications such as pulmonary artery rupture.⁵

One potential source of error is related to DICOM image registration from cardiac CT, as landmark points can vary due to observer interpretation or scan quality. Improvements in image acquisition and observers specialized in cardiac radiology can mitigate this barrier. Our study has demonstrated that the processing steps can be done with meaningful levels of accuracy. The results showed high correlation coefficients and infra-millimetric differences between the planimetric and photogrammetric method, which were not significant statistically. The results also revealed that the 3D printing of aortic valve models can be precise but with limitations related to inter-observer variability,⁶ which can lead to clinically important variations in geometry and dimensions. Potential sources of errors should be flagged to increase precision during the process of generating cardiovascular models. In our study, an important source of error was segmentation, as we encountered issues in delineating structures of interest and in using ROI tools such as dynamic grow mask or crop tools. However, further research, and particularly the use of AI, may improve semi-automatic functions and lead to the development of algorithms that delineate ROI more precisely. Other potential error sources were related to STL file processing and critical non-linear measurements on the 3D digital model. Digital analysis can mitigate these barriers using point cloud and mesh techniques, or colorimetric 3D maps when 3D-printed models are used.⁷

Another important limitation of our study is the fact that the entire process has been conducted by a single clinician.

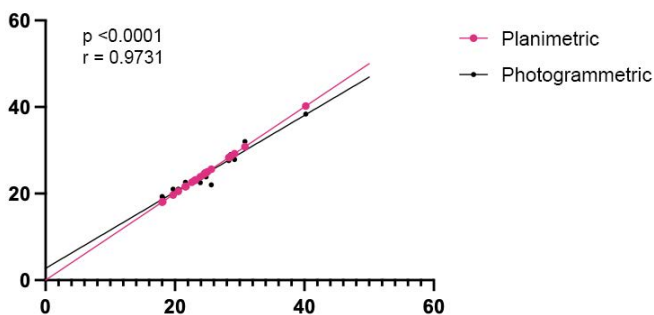


FIGURE 6. Correlation between the two measurement methods for the height of the sinus of Valsalva

In future studies, at least two observers should perform the image post-processing to identify key inter-observer differences. Furthermore, the number of patients included in the study was low. Increasing their number can decrease the risk of errors and improve the development of solutions regarding the workflow of 3D printing aortic valves.

In a study conducted by Fourie *et al.* on 3D models created from CT imagery, the authors observed important differences in the dimensions of 3D-printed models between clinicians and emphasized the importance of inter-observer errors and of semi-manual processing during the entire workflow.⁸ Furthermore, each stage in the process of 3D-printing a cardiovascular model is susceptible to errors. Similar results were obtained in a study conducted by Santana *et al.*, who observed discrepancies in the interpretation and subsequent analysis of medical images by different observers.⁹ Considering the continuous exposure to sources of error, it is mandatory to judiciously monitor potential errors generated by semi-automated processing. Cross-check points should be inserted in the intermediate stage, overlaying the generated digital model to original DICOM data presented in the current study. Future research is needed to determine the accuracy of 3D-printed aortic templates.¹⁰

CONCLUSIONS

In cardiovascular valve diseases, the precision of 3D-printed models is an important element that can contribute to increasing quality of procedural simulations and predicting potential complications. Various methods were studied for assessing the accuracy of 3D printing, each with strengths and weaknesses. The selected method of assessment may require a 3D-printing team with expertise in radiological field and in processing and post-processing of additive manufacture field.

CONFLICT OF INTEREST

Nothing to declare.

FUNDING

This work was supported by the “George Emil Palade” University of Medicine, Pharmacy, Science and Technology of Târgu Mureş Research Grant number 510/1/17.01.2022, and the Doctoral School of “George Emil Palade” University of Medicine, Pharmacy, Science and Technology of Târgu Mureş.

REFERENCES

1. Vukicevic M, Mosadegh B, Min JK, Little SH. Cardiac 3D Printing and its Future Directions. *JACC Cardiovasc Imaging*. 2017;10:171–184.
2. Levin D, Mackensen GB, Reisman M, McCabe JM, Dvir D, Ripley B. 3D Printing Applications for Transcatheter Aortic Valve Replacement. *Curr Cardiol Rep*. 2020;22:23.
3. Jiménez Restrepo A, Chahal D, Gupta A, et al. Roadmap to Success: 3D Printing in Pre-Procedural Planning. *J Am Coll Cardiol Case Rep*. 2020;2:358–360.
4. Cernica D, Benedek I, Polexa S, Tolescu C, Benedek T. 3D Printing-A Cutting Edge Technology for Treating Post-Infarction Patients. *Life (Basel)*. 2021;11:910.
5. Shirakawa T, Yoshitatsu M, Koyama Y, Mizoguchi H, Toda K, Sawa Y. 3D-printed aortic stenosis model with fragile and crushable calcifications for off-the-job training and surgical simulation. *Multimed Man Cardiothorac Surg*. 2018;2018.
6. Odeh M, Levin D, Inziello J, et al. Methods for verification of 3D printed anatomic model accuracy using cardiac models as an example. *3D Print Med*. 2019;5:6.
7. Nulty A. A comparison of trueness and precision of 12 3D printers used in dentistry. *BDJ Open*. 2022;8:14.
8. Fourie Z, Damstra J, Schepers RH, Gerrits PO, Ren Y. Segmentation process significantly influences the accuracy of 3D surface models derived from cone beam computed tomography. *Eur J Radiol*. 2012;81:e524–530.
9. Santana RR, Lozada J, Kleinman A, Al-Ardah A, Herford A, Chen JW. Accuracy of cone beam computerized tomography and a three-dimensional stereolithographic model in identifying the anterior loop of the mental nerve: a study on cadavers. *J Oral Implantol* 2012;38:668–676.
10. Rynio P, Wojtuń M, Wójcik Ł, Kawa M, Falkowski A, Gutowski P, Kazimierczak A. The accuracy and reliability of 3D printed aortic templates: a comprehensive three-dimensional analysis. *Quant Imaging Med Surg*. 2022;12:1385–1396.